

*In The Name of God, The Compassionate, The Merciful*

99121



Shiraz University  
Faculty of Engineering

**Ph.D. Dissertation In Civil Engineering**

**SHEAR MODULUS AND DAMPING RATIO OF MIXED  
GRAVEL AND CLAY**

By

**MAHRASHK MEIDANI**

Supervised by

**Prof. Arsalan Ghahramani  
Prof. Ghassem Habibagahi**

July 2008

۹۹/۱۲/۱

عزیز



دانشگاه شاهرز

دانشکده مهندسی

پایان نامه دکتری در رشته مهندسی عمران (مکانیک خاک و پی)

ضریب برشی و نسبت میرایی برای خاکهای مخلوط شنی  
رسی

توسط

مه رشک میدانی

استاد راهنما:

دکتر ارسلان قهرمانی

دکتر قاسم حبیب آگهی

۱۳۸۷ / ۷ / ۱۵

مرداد ماه ۱۳۸۷

۹۹۱۲۱

IN THE NAME OF GOD

**SHEAR MODULUS AND DAMPING RATIO OF MIXED GRAVEL AND  
CLAY**

BY

MAHRASHK MEIDANI

THESIS

SUBMITTED TO THE SCHOOL OF GRADUATE STUDIES IN PARTIAL FULFILLMENT  
OF THE REQUIREMENTS FOR THE DEGREE OF DOCTOR OF PHILOSOPHY (PH.D.)

IN

CIVIL ENGINEERING

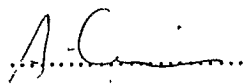
(SOIL MECHANICS AND FOUNDATION ENGINEERING)

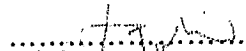
SHIRAZ UNIVERSITY

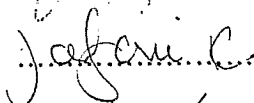
SHIRAZ

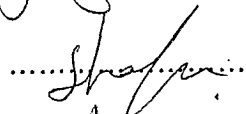
ISLAMIC REPUBLIC OF IRAN

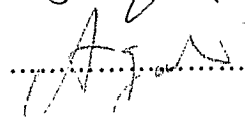
**EVALUATED AND APPROVED BY THE THESIS COMMITTEE AS: EXCELLENT**

 A. Ghahramani, Ph.D., Prof. of Civil Engineering (Chairman)

 G. Habibagahi, Ph.D., Prof. of Civil Engineering (Chairman)

 M.K. Jafari, Ph.D., Prof. of Civil Engineering

 A. Shafiee, Ph.D., Assistant Prof. of Civil Engineering

c/o  C.S. Chang, Ph.D., Prof. of Civil Engineering

JULY 2008

*Dedicated to My Beloved Parents.*

*Homa & Javad.*

## Acknowledgements

I would like to express my sincere thanks to my supervisors, Professor Arsalan Ghahramani and Professor Ghassem Habibagahi for their patient guidance throughout the period of my study in Shiraz University.

Cyclic triaxial tests were performed at the Advanced Soil Mechanics Laboratory of International Institute of Earthquake Engineering and Seismology (IIIES) in Iran. I would like to extend my deepest gratitude to my thesis advisors, Professor Mohammad Kazem Jafari and Dr. Ali Shafiee for granting unrestricted access to the laboratory resources and their fruitful discussions on my research details.

Special thanks to Eng. Mehdi Asgari, who helped me in setting up the triaxial devices in IIIES. I would like to thank Eng. Javad Jalili for developing the code for the analysis of raw data from the triaxial device. I also wish to thank other IIIES soil mechanics laboratory staff, Misters Mohammad-Kamran Shirazian, Shahriar Azadmanesh, Ebrahim Akbari, Saeed Yousefi and Ghassem Haadavi for their friendly cooperation during my stay in IIIES. The security personnel of IIIES had great cooperation with me during out-time stays in the laboratory.

Small strain monotonic triaxial tests were performed at the Soil Mechanics Laboratory, National Institute for Rural Engineering (NIRE) in Tsukuba, Japan. Without significant supports of Dr. Yoshiyuki Mohri, it was not possible to perform the tests in the period of my stay in Tsukuba. The helpful supports of Dr. Toshikazu Hori, Eng. Mitsuru Ariyoshi of NIRE, during the setup of tests is kindly acknowledged. Many thanks to the kind staff of NIRE, especially Mrs. Eiko Takahashi and Mrs. Yoshie Murata for their general supports during my stay in Tsukuba-shi.

I am particularly indebted to Eng. Afshin Naghshineh and Dr. Abdureza Fazeli and their kind families for their support during my stay in Shiraz city.

I had the opportunity to meet many great persons during my PhD course that influenced my vision in different aspects of life and study. Dr. Mohammad Taghi Izadi, Professor Ikuo Towhata, & Dr. Taro Uchimura from the University of Tokyo, Professor Leonardo Cascini from Salerno University, and my thesis advisor Professor Ching Shung Chang from the University of Massachusetts.

At last but not least, I want to thank my aunt, Ms. Mehrangiz Ghanimifard for her compassionate hospitality during my several stay periods in Tehran.

I dedicated my Ph.D degree to my mother and father with love.

Mahrashk Meidani  
July 2008; Shiraz, Iran

## ABSTRACT

# SHEAR MODULUS AND DAMPING RATIO OF MIXED GRAVEL AND CLAY

BY

MAHRASHK MEIDANI

Gravel-Clay mixtures are abundant material in nature and are frequently used in certain civil engineering projects such as earth dams, levees and landfills. The impervious core of Karkheh dam, one of largest earthdams in the world, is made of this material. The advantage of using these soils lies in their low permeability owing to clay fraction and high shear strength due the non-cohesive granular part. To date, little research has been carried out to investigate the performance of these soils and therefore, their behavior under cyclic loading is still not well known. In order to investigate the cyclic behavior of gravel-clay mixtures, 51 cyclic and monotonic triaxial tests were performed on specimens with 11 different mixtures and under various confining pressures. Two different types of gravel, i.e. angular and round grains, were utilized to prepare specimens with the same gravel content in order to investigate the effect of granule shape on the cyclic behavior of the mixture. A phenomenon called *contact crushing succeeded by granule slippage* is introduced for the angular gravels. The importance of sampling method and specimen size for intermediate soils is also noticed.

*Keywords: Cyclic Loading, Damping Ratio, Earthfill Dam, Granule Shape, Granule Contact, Gravel-Clay Mixture, Micromechanics, Shear Modulus.*

# Table of Contents

<i>Sec.</i>	<i>Title</i>	<i>Page</i>
<b>Chapter 1</b>	<b>Introduction</b>	<b>1</b>
1.1.	Opening	1
1.2.	Research plan and objectives	6
1.3.	Arrangement of dissertation	7
<b>Chapter 2</b>	<b>Literature Review</b>	<b>9</b>
2.1.	Introduction	9
2.1.1.	Overview	10
2.1.2.	Correlation of $G_{max}$ with other soil parameters	11
2.1.3.	$G/G_{max}$ - $\gamma$ relationships	11
2.1.4.	$D$ - $\gamma$ relationships	13
2.1.5.	Parameters Affecting $G$ and $D$ in soils	14
2.2.	Dynamic properties of gravelly soils	16
2.2.1.	Factors affecting the dynamic properties of granular soils at small strains	18
2.2.1.1.	Effects of void ratio and mean effective confining pressure on $G_{max}$ of sandy and gravelly soils	18
2.2.1.2.	Effects of gradation and particle shape on $G_{max}$ of granular soils	23
2.2.1.3.	Effect of Soil Disturbance on $G_{max}$ of Granular Soils	29
2.2.1.4.	Effect of Geologic Age on $G_{max}$ of Granular Soils	32
2.2.1.5.	Effect of Confining Pressure on Young's Modulus and Constrained Modulus of Granular Soils	33
2.2.1.6.	Small-Strain Material Damping Ratios in Shear of Granular Soils	37



<i>Sec.</i>	<i>Title</i>	<i>Page</i>
2.2.2.	Factors affecting the nonlinear dynamic properties in shear of gravelly soils	39
2.2.2.1.	Effect of Confining Pressure on Nonlinear Dynamic Properties in Shear of Gravelly Soils	40
2.2.2.2.	Effect of Disturbance on Nonlinear Dynamic Properties of Gravelly Soils	42
2.2.2.3.	Soils at Larger Strain Level ( $> 0.1\%$ )	43
2.2.2.4.	Soils given by Seed et al (1986)	45
2.3.	Analytical Models of Nonlinear Dynamic Soil Behavior in Shear	46
2.3.1.	Hyperbolic model by Hardin and Drnevich	46
2.3.2.	Modified hyperbolic model by Darendeli	47
2.3.3.	Ramberg-Osgood model by Anderson	49
2.4.	Analytical models of nonlinear dynamic soil behavior in cyclic shear	50
2.4.1.	Hyperbolic model by Hardin and Drnevich	51
2.4.2.	Modified hyperbolic model by Darendelli	52
2.4.3.	Ramberg-Osgood model by Anderson	52
2.4.4.	Masing behavior model for damping ratio by Ishihara	54
<b>Chapter 3</b>	<b>Resources of Research</b>	<b>56</b>
3.1.	Materials used in the laboratory tests	56
3.2.	Triaxial testing apparatus	62
3.2.1.	IIIES cyclic triaxial system	63
3.2.1.1	Main components	66
3.2.1.1.1.	Triaxial cell	66
3.2.1.1.2.	Loading piston	67
3.2.1.1.3.	Electro-pneumatic valve	67
3.2.1.1.4.	Signal generator and E.P. servo control unit	68
3.2.1.2.	Sensors	69
3.2.1.2.1.	Load cell	69
3.2.1.2.2.	Non-contact displacement transducer	70
3.2.1.2.3.	LVDT	70
3.2.1.2.4.	Pore water pressure transducer	71
3.2.1.2.5.	Volume change transducer	72

<i>Sec.</i>	<i>Title</i>	<i>Page</i>
3.2.1.3.	Other electronic components	72
3.2.1.3.1.	Analogue amplifiers	72
3.2.1.3.2.	ADC-DAQ-REC	73
3.2.2.	NIRE computer controlled triaxial system	73
3.2.2.1.	Main components of the NIRE triaxial system	74
3.2.2.1.1.	Triaxial cell	74
3.2.2.1.2.	Reaction frame	74
3.2.2.1.3.	Electric driving AC motor	74
3.2.2.2.	Sensors	78
3.2.2.2.1.	LVDT	78
3.2.2.2.2.	Load cell	78
3.2.2.2.3.	Pore water pressure transducer	79
3.2.2.2.4.	Volume change transducer	80
3.2.2.2.5.	Local displacement transducers (LDT)	80
3.2.2.3.	Other electronic components	83
3.2.2.3.1.	Analogue to digital converter and data acquisition system	83
3.2.2.3.2.	Loading system	83
3.2.2.3.3.	Electric Noise filter	83
3.2.2.3.4.	Analogue amplifier	83
<b>Chapter 4</b>	<b>Triaxial Tests</b>	<b>86</b>
4.1.	Sample preparation	86
4.2.	Tests setup	91
4.3.	Cyclic triaxial tests at IIEES	92
4.4.	Small strain CU tests at NIRE	93
<b>Chapter 5</b>	<b>Tests Results and Mathematical Modeling</b>	<b>95</b>
5.1.	Tests results and mathematical modeling for shear modulus	95
5.1.1.	Shear modulus versus shear strain	95
5.1.2.	G-gamma results from cyclic triaxial tests	98
5.1.2.1.	33.8% gravel content	98
5.1.2.2.	44.2% gravel content	98
5.1.2.3.	54.3% gravel content	99
5.1.2.4.	64.1% gravel content	100

<b>Sec.</b>	<b>Title</b>	<b>Page</b>
5.1.2.5.	73.5% gravel content	101
5.1.2.6.	Summary	102
5.1.3.	Maximum shear modulus	103
5.1.3.1.	small strain CU tests and maximum shear modulus	103
5.1.3.2.	Mathematical model for $G_{max}$	110
5.1.4.	Mathematical model for normalized shear modulus versus shear strain	111
5.1.4.1.	Darendelli model	112
5.2.	Results and discussion for damping ratio	126
5.2.1.	Damping ratio versus shear strain	126
5.2.1.1.	33.8% gravel content	126
5.2.1.2.	44.2% gravel content	126
5.2.1.3.	54.3% gravel content	127
5.2.1.4.	64.1% gravel content	128
5.2.1.5.	73.5% gravel content	129
5.2.2.	Mathematical model for damping ratio variation with shear strain	129
5.2.2.1.	Model D-1, polynomial function	130
5.2.2.2.	Model D-2, tangent-hyperbolic function	134
5.2.2.3.	Comparison between model D-1 and D-2	134
<b>Chapter 6</b>	<b>Conclusion and Future Research</b>	<b>145</b>
6.1.	Summary	145
6.2.	Conclusion	145
6.3.	Recommendation for future research	147
<b>References</b>		<b>148</b>

## List of Figures

<i>Sec.</i>	<i>Title</i>	<i>Page</i>
<b>Chapter 1 Introduction</b>		
1.1	Typical resonant column test apparatus: (a) top view of loading system, and (b) profile view of loading system and soil specimen (Kramer, 1996)	2
1.2	Typical triaxial apparatus for testing soil specimens (Kramer, 1996)	3
1.3	NGI cyclic simple shear apparatus (Kramer, 1996)	3
1.4	Typical stress-strain loops for the cyclic loading	4
1.5	idealized hysteresis loop in cyclic loading	5
1.6	Typical nonlinear $[G/G_{\max} - \log \gamma]$ and $[D_s - \log \gamma]$ curves for dry, medium-dense granular soils (Menq, 2002)	7
 <b>Chapter 2 Literature Review</b>		
2.1	Small strain shear modulus of tested sands (Lo Presti, 1997)	22
2.2	$G_{\max}$ as a function of effective confining pressure from resonant column tests (Schneider 1999)	23
2.3	Variation of $G_{\max}$ with effective confining pressure for the field deposits (Lin et al, 2000)	23
2.4	Relationship between effective confining pressure and $G_{\max}/F(e)$ (Chien, 2002)	24
2.5	Effect of the initial confining pressure on equivalent shear modulus (Teachavorasinskun, 2002)	24
2.6	Variation of small-strain shear modulus with void ratio of sandy and gravelly soils tested in Japan using the cyclic triaxial test (Ishihara, 1996)	25

<i>Sec.</i>	<i>Title</i>	<i>Page</i>
2.7	Gradation curves of sandy and gravelly materials tested in Japan (Ishihara, 1996)	26
2.8	Gradation of Denver sand specimens (Chang and Ko, 1986)	27
2.9	Small-strain shear modulus, $G_{\max}$ , versus uniformity coefficient, $C_u$ , at a mean effective confining pressure, $\sigma'_o$ , of 30 psi (2.0 atm) (after Chang and Ko, 1986)	27
2.10	Small-strain shear modulus, $G_{\max}$ , versus median grain size, $D_{50}$ , at a median effective confining pressure, $\sigma'_o$ , of 30 psi (2.0 atm) (after Chang and Ko, 1986)	28
2.11	Comparison of shear moduli from in situ and laboratory tests (Kokusho and Tanaka, 1994)	31
2.12	Gradation curves of specimens from four different sites in Japan (Kokusho and Tanaka, 1994)	31
2.13	Initial shear modulus versus mean effective confining pressure for intact sandy gravelly materials (Kokusho, 1987)	32
2.14	Variation of Sampling Disturbance Expressed in terms of $V_{s,lab}/V_{s,field}$ and $G_{\max,lab}/G_{\max,field}$ with the In-Situ Shear Wave Velocity (Darendeli, 2001)	33
2.15	$(K_2)_{\max}$ versus Relative Density, $D_r$ , for Holocene Gravels (Rollins et al., 1998)	34
2.16	$(K_2)_{\max}$ versus Relative Density ( $D_r$ ), for Pleistocene Gravels (Rollins et al., 1998)	34
2.17	Variation of Shear and Unconstrained Compression Wave Velocities with Isotropic Confining Pressure for Dry Ottawa Sand (after Hardin and Richart, 1963)	35
2.18	Diagrammatic Sketch of Experimental Set-Up for Seismic Wave Testing in LSTC (Lee, 1993)	37
2.19	Variation in P-Wave Velocities with Propagation Direction for Measurements in the Horizontal and Vertical Planes under Isotropic Loading (Lee, 1993)	38
2.20	Directions and Planes Associated with P-Wave Velocity Measurements Shown in Figure 2.19 (Lee, 1993)	38
2.21	Variation of Material Damping Ratio in shear with Strain Amplitude and Confining Pressure of Pea-Gravel (Wu, 1986)	39

<i>Sec.</i>	<i>Title</i>	<i>Page</i>
2.22	Variation of Material Damping Ratio with Confining Pressure of Dry Washed Mortar Sand (Laird, 1994)	40
2.23	Effect of effective isotropic confining pressure on $G/G_{\max}$ - $\log \gamma$ and $D$ - $\log \gamma$ curves of reconstituted gravelly materials (Tanaka et al., 1987)	42
2.24	Variation of Reference Shearing Strain, $\gamma_p$ , with Effective Isotropic Confining Pressure (Tanaka et al., 1987)	42
2.25	Comparisons of Nonlinear Properties between Intact and Reconstituted Specimens of Tokyo Gravel (Hatanaka and Uchida, 1995)	44
2.26	Effect of Sample Disturbance on $G/G_{\max}$ - $\log \gamma$ Relation of Gravelly Material from Site K (Kokusho and Tanaka, 1994)	44
2.27	Gradation Curves of Four Gravelly Soils Tested by Lin et al. (2000) along with In-Situ Gradation Curve	45
2.28	Effect of Gravel Content on Normalized Shear Modulus Curves at Large Strain (Lin et al., 2000)	46
2.29	$G/G_{\max}$ - $\log \gamma$ Curves of Gravelly and Sandy Soils Suggested by Seed et al. (1986)	47
2.30	$D$ - $\log \gamma$ Curves of Gravelly and Sandy Soils Suggested by Seed et al. (1986)	47
2.31	Modulus reduction curves for fine grained soils of different plasticity (Kramer, 1996)	49
2.32	Influence of mean effective confining pressure on modulus reduction curves for (a) non-plastic soil, and (b) plastic soil (PI=50). (Kramer, 1996)	50
2.33	Effect of cyclic degradation on shear modulus (Kramer, 1996)	51
2.34	Variation of damping ratio of fine grained soils with cyclic shear strain amplitude and plasticity index (Kramer, 1996)	52
2.35	Hyperbolic backbone curve asymptotic to $\tau = G_{\max} \gamma$ and to $\tau = \tau_{\max}$	53
2.36	Comparisons between Ramberg-Osgood and Hyperbolic models (Kagawa, 1992)	56
2.37	Relation between Material Damping Ratio and Normalized Shear Modulus (Hwang, 1997)	57

<i>Sec.</i>	<i>Title</i>	<i>Page</i>
2.38	Relation between Material Damping Ratio and Normalized Shear Modulus (Ishihara, 1996)	58

### **Chapter 3. Resources of Research**

3.1	Grading curves for materials used in this study	56
3.2	Results of Casagrande test on clay material used in this study	57
3.3	Compaction curve for clay material used in the tests	57
3.4	Selection of proper granules for the tests from gravel mass	58
3.5	A typical round granule used in this study	59
3.6	A typical round granule used in this study	59
3.7	A typical round granule used in this study	60
3.8	A typical angular granule used in this study	60
3.9	A typical angular granule used in this study	61
3.10	A typical angular granule used in this study	61
3.11	A typical angular granule used in this study	62
3.12	Panorama view of the cyclic triaxial testing system in IIEES, Tehran	64
3.13	Simplified cyclic triaxial testing apparatus diagram for IIEES apparatus	65
3.14	Triaxial cells with soil specimens under consolidation	66
3.15	Loading piston installed on the cyclic loading frame	67
3.16	Schematic drawing of electropneumatic valve and loading piston connected to it	68
3.17	Electropneumatic valve and its components on the loading table	68
3.18	Signal generator and E.P. servo controller unit	69
3.19	Submersible load cell installed inside the triaxial cell (IIEES)	69
3.20	Noncontact displacement transducer installed inside the triaxial cell	70
3.21	LVDT installed outside the triaxial cell	71
3.22	Pore water pressure transducer with de-airing valve	71
3.23	Volume change transducer connected to the bottom of burette	72
3.24	Eight analogue amplifiers side by side on the main control panel	73
3.25	TEAC DR-F3 digital recorder device	73
3.26	NIRE triaxial cell and loading frames	75
3.27	NIRE triaxial testing apparatus diagram	76

<i>Sec.</i>	<i>Title</i>	<i>Page</i>
3.28	AC electric motor and loading components	77
3.29	A planetary gear and its components	77
3.30	Relationship between driving motor speed and axial displacement rate in the triaxial device	77
3.31	LVDT installed on the triaxial cell (NIRE)	78
3.32	Load cell installed at the bottom of loading ram and above top cap (NIRE)	79
3.33	Pore water pressure transducer (NIRE)	79
3.34	Volume change transducer connected to the burette	80
3.35	An LDT installed on the sample	81
3.36	Details of LDT and its proper installation on the sample	82
3.37	14bit Keyence Corp. data acquisition system, NR-250	83
3.38	Data acquisition system on top and its input terminal board, AC motor and clutch system switch panels	84
3.39	Industrial laptop; load control system and noise filter, analogue amplifier	85

#### **Chapter 4 Triaxial Tests**

4.1	Trial sample to check the uniform density of the sample after undercompaction	89
4.2	The aluminum mold and hammer used to prepare the specimens for cyclic testing	90
4.3	100% clayey sample, 44.2% angular gravelly sample and 73.5% angular gravelly sample out of the mold	91
4.4	Steps followed for sample preparation and testing of specimens	92
4.5	Two specimens placed in the triaxial cell during consolidation stage	93
4.6	Definition of bedding error in the measurement of initial small displacement	94

#### **Chapter 5 Tests Results and Mathematical Modeling**

5.1	A magnified view of the angular granules and clay showing many empty voids at 73.5% gravel content	97
5.2	Internal friction angle of specimens with the same gravel content compacted with the same effort	97



<i>Sec.</i>	<i>Title</i>	<i>Page</i>
5.3	Shear modulus versus shear strain amplitude for samples with 33.8% gravel content and clay samples under different effective confining pressures	98
5.4	Shear modulus versus shear strain amplitude for samples with 44.1% gravel content and clay samples under different effective confining pressures	99
5.5	Shear modulus versus shear strain amplitude for samples with 54.3% gravel content and clay samples under different effective confining pressures	100
5.6	Shear modulus versus shear strain amplitude for samples with 64.1% gravel content and clay samples under different effective confining pressures	101
5.7	Shear modulus versus shear strain amplitude for samples with 73.5% gravel content and clay samples under different effective confining pressures	102
5.8	Stress-strain curve for test a511 at very small strains range	104
5.9	Stress-strain curve for test a533 at very small strains range	104
5.10	Stress-strain curve for test a555 at very small strains range	104
5.11	Stress-strain curve for test a611 at very small strains range	105
5.12	Stress-strain curve for test a633 at very small strains range	105
5.13	Stress-strain curve for test a655 at very small strains range	105
5.14	Stress-strain curve for test a711 at very small strains range	106
5.15	Stress-strain curve for test a733 at very small strains range	106
5.16	Stress-strain curve for test a755 at very small strains range	106
5.17	Stress-strain curve for test r511 at very small strains range	107
5.18	Stress-strain curve for test r533 at very small strains range	107
5.19	Stress-strain curve for test r555 at very small strains range	107
5.20	Stress-strain curve for test r611 at very small strains range	108
5.21	Stress-strain curve for test r633 at very small strains range	108
5.22	Stress-strain curve for test r655 at very small strains range	108
5.23	Stress-strain curve for test r711 at very small strains range	109
5.24	Stress-strain curve for test r733 at very small strains range	109
5.25	Stress-strain curve for test r755 at very small strains range	109
5.26	Predicted vs. measured normalized shear modulus	111
5.27	Darendelli model constant constants obtained from preliminary optimization	114

<i>Sec.</i>	<i>Title</i>	<i>Page</i>
5.28	Predicted vs. measured values of normalized shear modulus for initial model and final model	115
5.29	Normalized shear modulus vs. shear strain for samples with 54.3% angular gravel , and predicted vs. measured values	116
5.30	Normalized shear modulus vs. shear strain for samples with 64.1% angular gravel , and predicted vs. measured values	117
5.31	Normalized shear modulus vs. shear strain for samples with 73.5% angular gravel , and predicted vs. measured values	118
5.32	Normalized shear modulus vs. shear strain for samples with 54.3% round gravel , and predicted vs. measured values	119
5.33	Normalized shear modulus vs. shear strain for samples with 64.1% round gravel , and predicted vs. measured values	120
5.34	Normalized shear modulus vs. shear strain for samples with 73.5% round gravel , and predicted vs. measured values	121
5.35	Comparison between normalized shear modulus values for angular and round gravel mixtures at certain gravel contents	123
5.36	Comparison between normalized shear modulus values at different gravel contents for angular and round gravel mixtures	124
5.37	The hypothesized mechanism of granules slippage during cyclic shear between round granules	125
5.38	The hypothesized mechanism of angular granules breakage at contact level succeeded by slippage	125
5.39	Damping ratio values for 100% clay samples and specimens with 33.8% gravel	126
5.40	Damping ratio values for 100% clay samples and specimens with 44.2% gravel	127
5.41	Damping ratio values for 100% clay samples and specimens with 54.3% gravel	127
5.42	Damping ratio values for 100% clay samples and specimens with 64.1% gravel	128
5.43	Damping ratio values for 100% clay samples and specimens with 73.5% gravel	129
5.44	Damping ratio vs. shear strain amplitude for the samples with 54.3% angular gravel content at different effective confining pressures, and predicted vs. measured graph for model D-1	131

<i>Sec.</i>	<i>Title</i>	<i>Page</i>
5.45	Damping ratio vs. shear strain amplitude for the samples with 64.1% angular gravel content at different effective confining pressures, and predicted vs. measured graph for model D-1	131
5.46	Damping ratio vs. shear strain amplitude for the samples with 73.5% angular gravel content at different effective confining pressures, and predicted vs. measured graph for model D-1	132
5.47	Damping ratio vs. shear strain amplitude for the samples with 54.3% round gravel content at different effective confining pressures, and predicted vs. measured graph for model D-1	132
5.48	Damping ratio vs. shear strain amplitude for the samples with 64.1% angular gravel content at different effective confining pressures, and predicted vs. measured graph for model D-1	133
5.49	Damping ratio vs. shear strain amplitude for the samples with 73.5% angular gravel content at different effective confining pressures, and predicted vs. measured graph for model D-1	133
5.50	Damping ratio vs. shear strain amplitude for the samples with 54.3% angular gravel content at different effective confining pressures, and predicted vs. measured graph for model D-2	135
5.51	Damping ratio vs. shear strain amplitude for the samples with 64.1% angular gravel content at different effective confining pressures, and predicted vs. measured graph for model D-2	136
5.52	Damping ratio vs. shear strain amplitude for the samples with 73.5% angular gravel content at different effective confining pressures, and predicted vs. measured graph for model D-2	137
5.53	Damping ratio vs. shear strain amplitude for the samples with 54.3% round gravel content at different effective confining pressures, and predicted vs. measured graph for model D-2	138
5.54	Damping ratio vs. shear strain amplitude for the samples with 64.1% round gravel content at different effective confining pressures, and predicted vs. measured graph for model D-2	139
5.55	Damping ratio vs. shear strain amplitude for the samples with 73.5% round gravel content at different effective confining pressures, and predicted vs. measured graph for model D-2	140
5.56	Comparison between damping ratio values of the mixtures with different gravel contents along with model D-2 predictions, Angular gravel, Round gravel	142

<i>Sec.</i>	<i>Title</i>	<i>Page</i>
5.57	Comparison between damping ratio values of the mixtures with different gravel type along with model D-2 predictions, 54.3% gravel content, 64.1% gravel content, 73.5% gravel content	143
5.58	Predicted vs. measured damping ratio values for both D-1 and D-2 models	144